Volume 27
Number 34
14 September 2025
Pages 10037-10276

Green Chemistry

Cutting-edge research for a greener sustainable future

rsc.li/greenchem

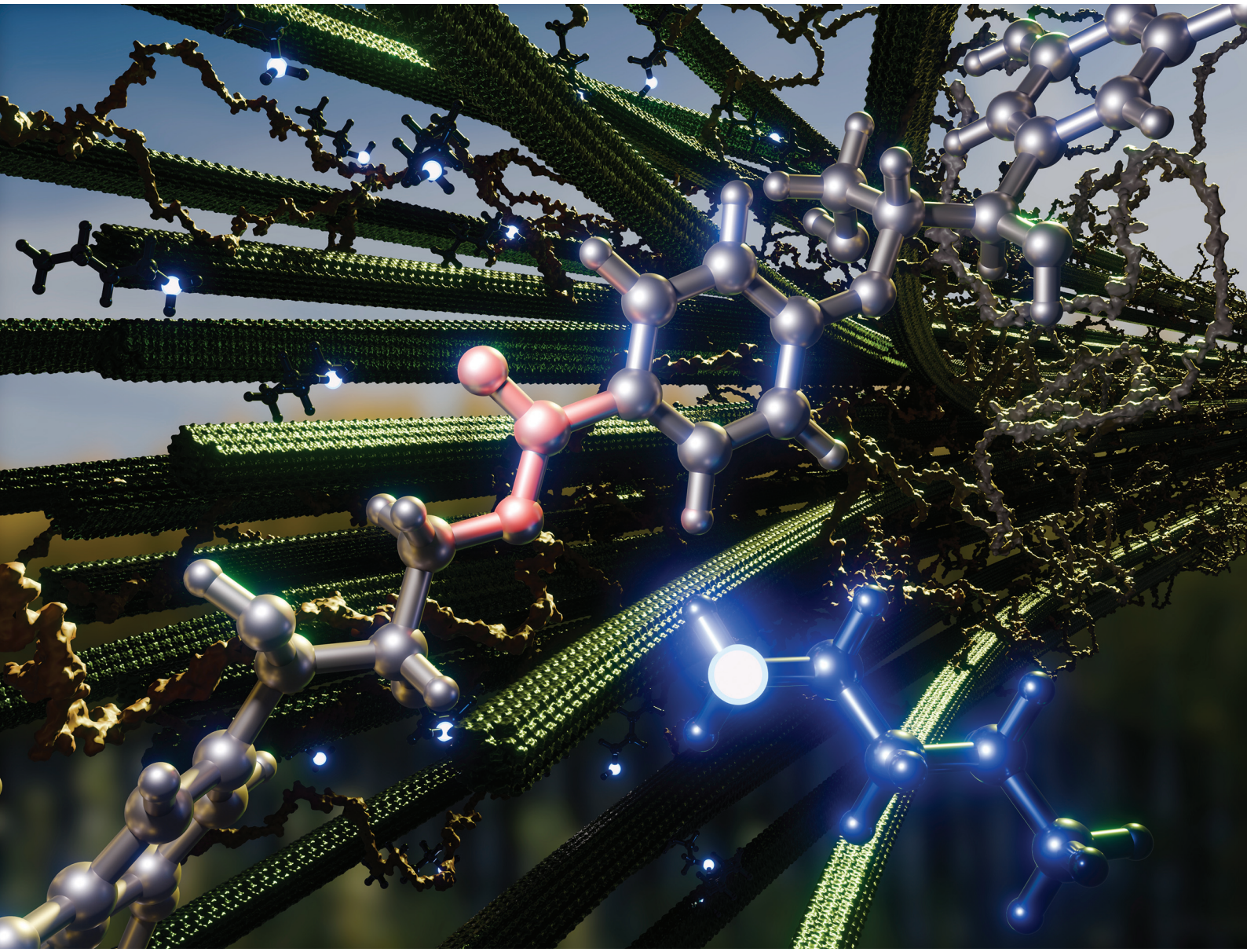

ISSN 1463-9262

ROYAL SOCIETY OF CHEMISTRY

PAPER
Blake A. Simmons *et al.*
The importance of ester cleavage in the butylamine pretreatment of hybrid poplar

25 YEARS ANNIVERSARY

Green Chemistry

PAPER

View Article Online
View Journal | View Issue

Cite this: *Green Chem.*, 2025, **27**, 10117

The importance of ester cleavage in the butylamine pretreatment of hybrid poplar†

Joseph M. Palasz,[a] Anagha Krishnamoorthy,[a] Raynald A. Giovine,[b] Xueli Chen,[a] Venkataramana Pidatala,[a,c] Emine A. Turumtay,[a,c] Tyrell S. A. Lewis,[d] Edward E. K. Baidoo,[a,c] Chang Dou,[d] Hemant Choudhary,[c,e] Ning Sun[d] and Blake A. Simmons*[a,c]

This work explores the "in-and-out" pretreatment of hybrid poplar with butylamine as a distillable protic solvent and reagent. The butylamine solvent can be removed by vacuum distillation with >95% solvent removal in all cases, providing a valuable scheme for efficient solvent recovery and recycling. Running the reaction with neat butylamine at 140 °C for 3 hours results in high yields of monosaccharides (90% glucose and 71% xylose) after enzymatic digestion, and a good tolerance to water content with no significant reduction in glucose yield up to an 8 : 1 water : butylamine ratio. We investigate the mechanisms of this pretreatment using powder X-ray diffraction, thermogravimetric analysis, fluorescence microscopy, elemental analysis, solid state and solution state nuclear magnetic spectroscopy to observe chemical and material markers of the pretreatment chemistry. The results suggest that the butylamine leaves the macro and microstructural properties of the lignocellulose relatively unaltered, but conducts targeted ester cleavage chemistry to remove cross-links between the various biopolymers and partially solubilize the lignin component of the biomass. These findings should act to guide future development of pretreatment chemistry for the development of biorefinery processes, and assist in the utilization of biomass as a starting point for chemical syntheses.

Received 11th April 2025,
Accepted 16th May 2025

DOI: 10.1039/d5gc01795e

rsc.li/greenchem

Green foundation

1. This work makes significant contributions to advancing sustainable biofuel production through the demonstration of protic amine solvents that can be efficiently recovered after biomass pretreatment.
2. Running the reaction with neat butylamine results in high yields of monosaccharides (90% glucose and 71% xylose) after enzymatic digestion, and a good tolerance to water content.
3. It is recommended that future work be focused on developing closed-loop solvent systems with near-100% recovery efficiency. This would include exploring alternative solvent recovery methods, such as membrane separation or adsorption techniques.

Introduction

As we pursue modernizing our chemical and energy production to efficiently utilize agricultural and forestry waste biomass, it is important to develop efficient conversion technologies for unlocking the potential of these biomass based resources. It has been estimated that there can be more than 1 billion tons of non-food lignocellulosic biomass produced annually in the United States alone.[1,2] Non-food waste biomass is of particular interest because most is discarded or burned for energy. Unlocking that biomass for the production of fuels, materials and chemicals will allow us to supply industries from wherever plants grow.

The vast majority of waste biomass occurs in the form of lignocellulose, which is an assembly of three biopolymers; cellulose, hemicellulose and lignin. As polysaccharides, the cellulose and hemicellulose fractions can be utilized to generate sugars for microbial fermentations. These bioprocesses can produce a variety of valuable products, including certain high-

[a]*Biological Systems and Engineering Division, Lawrence Berkeley National Laboratory, Berkeley, CA 94720, USA. E-mail: basimmons@lbl.gov*
[b]*Pines Magnetic Resonance Center (PMRC) – Core Facility, College of Chemistry, University of California, Berkeley, CA 94720, USA*
[c]*Joint BioEnergy Institute, Emeryville, CA 94608, USA*
[d]*Advanced Biofuels and Bioproducts Process Development Unit, Lawrence Berkeley National Laboratory, Emeryville, CA 94608, USA*
[e]*Department of Bioresource and Environmental Security, Sandia National Laboratories, Livermore, CA 94550, USA*

† Electronic supplementary information (ESI) available. See DOI: https://doi.org/10.1039/d5gc01795e

interest aviation fuel precursors.[3–6] While the enzymatic depolymerization of the cellulose and hemicellulose components is well developed.[7] The lignocellulose still requires chemical or physical pretreatment for the enzymes to gain access to the polysaccharide components of the biomass.[8,9] While fermentation derived bioprocesses based on lignocellulose conversion include several biology focused technologies, the pretreatment of lignocellulose to enable those downstream operations is fundamentally a materials and chemistry problem.

Many biomass pretreatment technologies have been explored over several decades, and many such approaches have resulted in efficient sugar release from a wide variety of potential bio-energy feedstocks. The scalability necessary for fuel and platform chemical production has prevented many of the contemporary pretreatment technologies from being cost-effective. The energy, hardware and reagent costs of pretreatment are of paramount importance in the viability of any lignocellulose derived process at scale.[10,11] To substantially reduce these costs, as well as the potential safety impacts of large-scale biomass pretreatment, it is important to develop pretreatment reagents and solvents which can be recycled in a closed-loop system where a small volume of solvent can be continuously recycled to treat a much larger quantity of biomass over time.

Alkaline pretreatments of lignocellulosic biomass are widely studied as they can enable selective lignin and hemicellulose dissolution.[12,13] These alkaline pretreatments have been found to operate with a variety of mechanisms including the disruption of crystalline cellulose, the dissolution and removal of lignin and the deacylation of the various ester functionalities. However, the use of mineral bases, while common, requires expensive recovery steps.[14] Ammonia gas, aqueous ammonia, and alkylamines are examples of alkaline reagents that can greatly simplify the pretreatment solvent recovery and recycle process and enable an "in-and-out" approach to lignocellulose deconstruction yielding dry pretreated biomass with no carbon losses.[12,15–19] Alkylamines in particular have started to appear as effective pretreatment reagents which combine some of the effects of organosolv and alkaline processes.[21,22] Alkanolamines have recently been explored as reactive solvents with very promising results.[23,24] Butylamine was originally explored by Tanaka *et al.* for the pretreatment of corn stover.[25] As a simple alkylamine (pK_a ~10.7) with intermediate polarity and boiling point (78 °C), it is a good starting point in terms of molecular identity to explore the underlying mechanisms of alkylamine based pretreatments following an in-and-out pretreatment scheme.

Hybrid poplar has been identified as a potential high-yielding bioenergy crop due to its high productivity and ability to regrow from trunks after harvest.[26] Hardwoods (and more generally eudicots) represent a promising but difficult class of lignocellulose to unlock due to their tightly interwoven structure and high lignin content when compared to more common grassy feedstocks (*e.g.* corn stover, sugarcane begasse).[19,27] As a hardwood, hybrid-poplar possesses syringyl rich lignin with monolignol conjugates of *p*-hydroxybenzoate

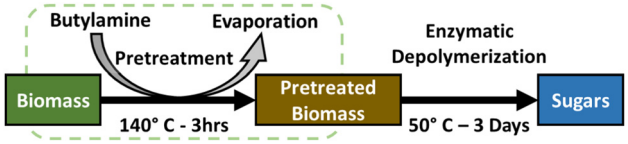

Scheme 1 Schematic of the in-and-out pretreatment process explored within this work. The process involves an initial pretreatment step with butylamine at elevated temperature, followed by evaporative drying to yield a dry solid which is efficiently digested by a cellulase/hemicellulase enzyme cocktail to monomeric sugars.

which play a significant, but unidentified, structural role in their cell-walls. The work herein studies samples of a hybrid poplar clone which is a cross between *Populus deltoides* and *Populus nigra* as a potentially valuable feedstock for bioenergy and bioproduct processes.

This work explores a pretreatment protocol on hybrid poplar using butylamine as an alkaline reagent and protic solvent that can be removed by distillation, thereby eliminating the losses of soluble sugars and small molecules (Scheme 1). We also explore the reaction space of butylamine pretreatment to understand how conditions such as water content and atmosphere influence the efficacy of the pretreatment process. We investigate the mechanisms of this pretreatment with powder X-ray diffraction (pXRD), thermal gravimetric analysis (TGA), fluorescence microscopy, solution and solid state nuclear magnetic resonance (NMR) spectroscopy to identify the material and chemical changes that occur during pretreatment in the structure of poplar. We maintain a specific focus on unravelling those cross-linking moieties within biomass that are chemically attacked by the butylamine pretreatment, with the aims of informing lignocellulose chemistry towards more selective, facile and scalable processes.

Results and discussion

The in-and-out pretreatment of hybrid poplar with butylamine

To begin exploring the activity of butylamine as an in-and-out pretreatment solvent for hybrid poplar, we first assessed our hybrid poplar biomass samples following the NREL compositional analysis protocol.[28] We chose to use the pretreatment conditions of 140 °C for three hours with a 15% solid biomass loading as an intermediate baseline condition. The results of both compositional analysis of hybrid poplar and the pretreatment runs are shown in Fig. 1. The sample has a glucan content of 45 ± 0.4%, with a total lignin content of 29.0 ± 0.1% and xylan content of 16.8 ± 0.1% demonstrating this sample of hybrid poplar may be a compelling source of glucose and lignin fractions.

We first tested the influence of varying solvent composition during pretreatment in glass pressure tubes. Under the tested conditions the butylamine pretreatment performed well both as a neat solvent and as an additive in an aqueous solution, yielding >84% glucose release in all test cases with neat butyla-

Compositional Analysis of Hybrid Poplar (% of dry weight)

Glucan	Xylan	Klason Lignin	Acid Soluble lignin	Residual Moisture	Ash
45.0 ± 0.4 %	16.8 ± 0.1%	23.9 ± 0.1%	5.1 ± 0%	9.48 ± 0.44%	0.7 ± 0.2%

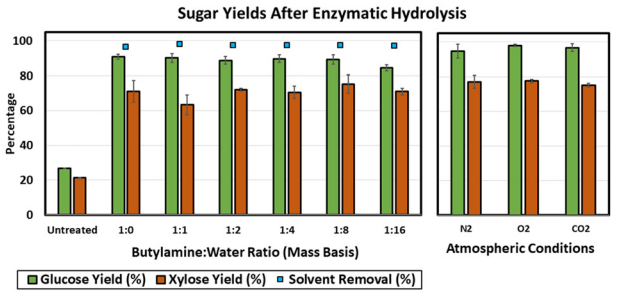

Fig. 1 The NREL compositional analysis of the hybrid poplar sample used in this study reported in percentages of the total dry-weight of the biomass (top) and the recovered sugar yields achieved following pretreatment and enzymatic hydrolysis of hybrid poplar with varying pretreatment conditions (bottom).

mine yielding the most glucose at 90.76 ± 1.50% yield. Untreated hybrid poplar yielded a modest 26.9 ± 0.13% glucose and 21.27 ± 0.19% xylose. Only in the 1 : 16 butylamine to water ratio was there a significant loss in glucose compared to neat butylamine with the yield dropping to 84.44 ± 1.70%. This is a promising result as it indicates the butylamine pretreatment is tolerant of relatively substantial quantities of water, which may eliminate the need for multiple costly drying steps in a potential biorefinery scheme. The xylan yields varied more substantially, however yields remained about 60% in all cases.

To test the influence of atmospheric composition on the butylamine pretreatment reaction we ran the same pretreatment conditions with 15% solid loading of hybrid poplar with neat butylamine in 75 mL Parr reactors with N_2, O_2 and CO_2. The glucose yields for N_2, O_2 and CO_2 were 94.51 ± 4.1%, 97.86 ± 0.51% and 96.51 ± 2.26% respectively. Unfortunately transfer losses from the Parr reactors prevented the collection of meaningful solvent removal data, although the samples were still extensively dried. The samples ran under a CO_2 atmosphere appeared fully solid after cooling, which was likely due to reactions between CO_2 and butylamine. Surprisingly, this did not meaningfully affect the sugar yields. The increase in glucose yield across all three samples is attributed to the superior mixing and heat transfer in the parr reactor compared to the prior runs which were conducted in glass pressure tubes. The minimal difference in sugar release with varying atmospheric conditions suggests that the presence of oxygen does not substantially influence the outcome of the pretreatment event, indicating oxidative lignin depolymerization is not a significant contributor to this process. The tolerance to a CO_2 atmosphere allows us to envisage a scheme where the reactivity of amines as pretreatment solvents and alkaline scrubbing reagents may be utilized simultaneously.

Overall these results demonstrated promising sugar yields and established that butylamine is a relatively resilient reagent for pretreatment of hybrid poplar, retaining its activity in a wide variety of concentrations and atmospheric conditions. As butylamine is a simple amine, we felt it would be prudent to investigate how butylamine altered the structure of the lignocellulose to enable this heightened activity of the subsequent enzymatic digestion steps.

The mechanism of butylamine pretreatment

Since this pretreatment scheme seems both effective and simple, we chose to pursue some mechanistic characterization to provide insight into how the butylamine pretreatment alters the structure of the biomass. From this point we chose to focus on pretreatment with 100% butylamine under ambient atmosphere. While the sugar yields of aqueous amine pretreatments are consistently high, we suspected that the inclusion of water in the pretreatment system may complicate the reaction pathways, and make it more difficult for us to identify the important mechanism of this pretreatment.

As lignocellulose is first, and foremost, a material, we started with several material characterization techniques to observe the changes during pretreatment. Since the primary structural component of plan cell walls are crystalline fibers of cellulose, pXRD has been a valuable tool for assessing whether the cellulose matrix has been altered.[29,30] Many pretreatment approaches, including ionic liquid, ammonia and soda pulping report substantial changes to the cellulose crystallinity and suggest that it is an essential operation in those pretreatment reactions.[31–33] Contrasting that precedent, the butylamine pretreated hybrid poplar samples showed a near identical pXRD pattern, suggesting that the morphology of the cellulose remains relatively unaltered (Fig. 2A). Thermogravimetric decomposition measurements of lignocellulose have been used to assess changes to both composition[34] and cellulose order.[35] We employed TGA and the resulting first derivative DTG curve (Fig. 2B) as a secondary technique to assess the how butylamine pretreatment altered the biomass. The TGA curves of untreated and pretreated hybrid-poplar are again similar, showing only a modest change in the shape and peak temperature of the crystalline cellulose decomposition peak near 350 °C.

To add further qualitative characterization we utilized the autofluorescence of the lignin under fluorescence microscopy to image the hybrid poplar before (Fig. 2C) and after pretreatment (Fig. 2D). The biomass particles did not noticeably change size, nor lose the microstructure of the cell wall ordering, further validating the assertion that the butylamine pretreatment is not altering the material structure or ordering of the cell walls. There was a clear change in the level of contrast in the samples after pretreatment, suggesting that the fluorescent lignin component is being modified or relocated within the biomass during the pretreatment and evaporation process. These results demonstrated that very modest changes to the material properties of the lignocellulose are sufficient to achieve the goal of increasing enzyme accessibility to the

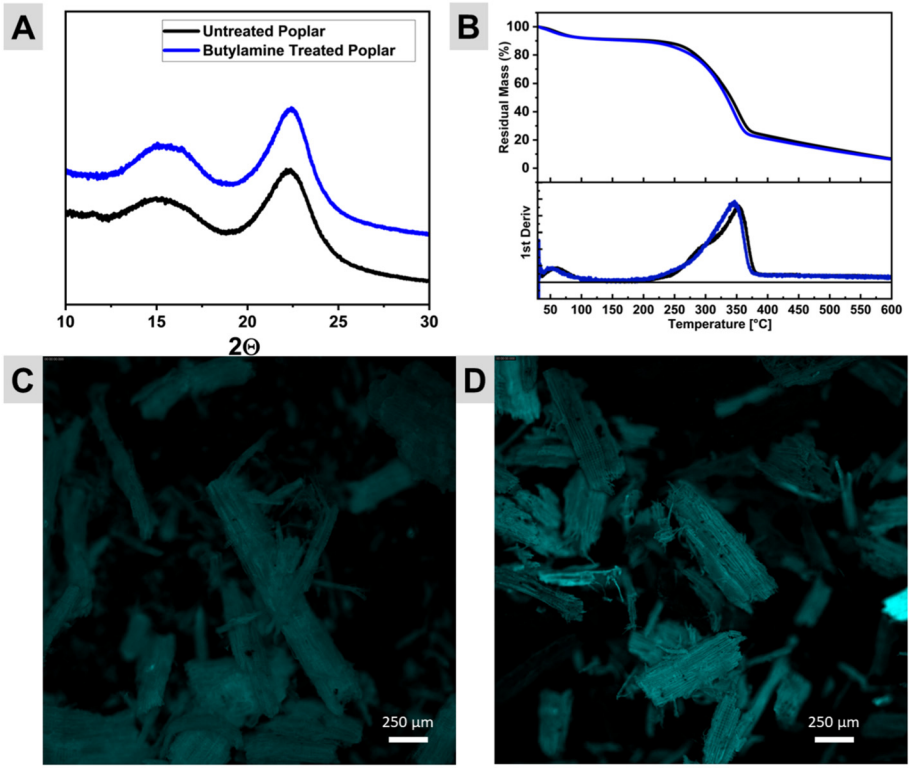

Fig. 2 pXRD spectra (A) of untreated (black) and butylamine pretreated (blue) hybrid poplar samples, TGA (B) of untreated (black) and butylamine pretreated (blue) hybrid poplar samples, and fixed-contrast fluorescence microscopy images of untreated (C) and pretreated (D) milled particles of hybrid poplar.

biomass. This specificity implies that only a few chemical operations may be necessary for high-yielding pretreatment, and may be possible to achieve in more facile conditions if those modifications can be identified.

To start exploring the chemical changes which have occurred in the pretreated biomass, we used cross-polarization magic-angle-spinning (CP-MAS) solid state nuclear magnetic resonance (ssNMR) spectroscopy. When sufficiently ball-milled to a fine particle size, lignocellulosic biomass can be packed into a 4 mm ssNMR rotor and yield sufficient signal to obtain an informative ^{13}C CP-MAS spectra. The ^{13}C CP-MAS spectra for untreated hybrid poplar, butylamine pretreated hybrid poplar and the solid residual after the enzymatic hydrolysis step are shown in Fig. 3. In further confirmation of the previous materials characterization, the CP-MAS spectra of both untreated and pretreated hybrid poplar are strikingly similar. While not quantitative, peaks attributable to cellulose dominate the spectra for both untreated and butylamine pretreated biomass, reflecting the principal component in the biomass. A small, but noticeable, peak attributable to acyl carbon functionalities is a present around ~173 ppm in the untreated biomass, which broadens into the baseline in the pretreated spectra, alluding to, but not confirming the modification of acyl carbon functionality during pretreatment. The most stark difference between the untreated and pretreated biomass is the presence of peaks attributable to the butylamine alkyl

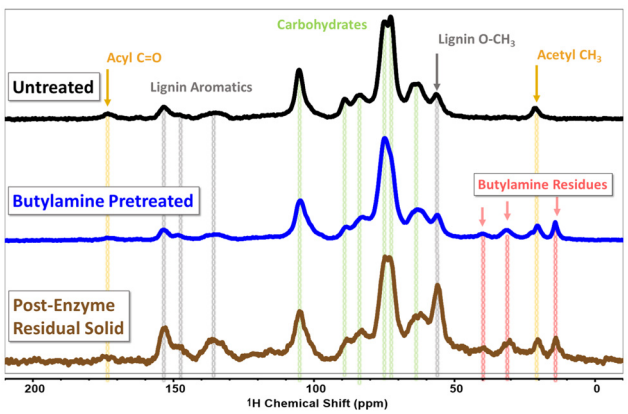

Fig. 3 Solid state ^{13}C CP-MAS NMR spectra of untreated (black, top) butylamine pretreated (blue, middle) and the lignin-rich solid residual after enzymatic saccharification (brown, bottom). Peaks assigned to carbohydrate (cellulose and hemicellulose) are marked with green vertical lines. Peaks associated with lignin aromatic moieties are marked with grey lines. Peaks associated with the butyl chain of butylamine are marked with pink lines and peaks associated with acetyl or acyl carbons are marked with yellow.

chain in the 10–50 ppm region of the pretreated biomass. This indicates some inclusion of butylamine groups in the pretreated solid. We suspect some quantity of butylamine reacts *via* acid–base reactions to form non-volatile butylammonium

salts with the carboxylate and phenolate functional groups present in the biomass, as well as with cleaved acetate functionalities resulting in butylammonium acetate. We also expected some chemical derivatization of the biomass through amidation and amination reactions which have been shown to occur in ammonia and other amine based pretreatments. The residual solid after enzymatic hydrolysis clearly shows a higher intensity of the aromatic lignin peaks in the as well as the aryl methoxy peak at ~55 ppm indicating an enrichment of lignin within the residue. Peaks in the carbohydrate region remain in residual solid, reflecting incomplete depolymerization of the polysaccharides,[36] or some residual lignin–carbohydrate complexes which have prevented complete digestion.[37] Relative to the lignin aromatic signals appearing from 130–160 ppm, the butylamine derived signals in the 10–40 ppm region decrease in intensity in the residual solid. We take this to indicate that some of the butylamine functionalized species may be water soluble and removed with the aqueous hydrolysate. This may present an issue for fermentation processes if the sugar-rich hydrolysate stream contains butylamine functionalized small-molecules and oligomers.

While we could observe the presence of butylamine residues within the pretreated biomass, we wanted to understand what moieties within the biomass were functionalized. Solution-state NMR can provide information about the chemical linkages present within biomass and has been a valuable tool for the identification of linkages present in the lignin and hemicellulose fractions.[38] To start we chose to study the DMSO extracts of untreated and pretreated biomass. DMSO is a strong polar solvent which can dissolve both lignin and some polysaccharide components of biomass, and is widely available in deuterated form.

Unsurprisingly, the extraction of untreated biomass with DMSO-d_6 yielded no identifiable soluble products. The pretreated biomass visibly released a dark brown extract. The absence of soluble components in the raw biomass is likely due to the tightly interconnected character of the lignocellulose. This may include various covalent and mechanical crosslinks between the various biopolymer components. In the ^{13}C NMR spectra of the pretreated extract, the major component is *N*-butylacetamide which we suspect is derived from amidation reactions cleaving acetyl groups in the biomass.

The ^{1}H–^{13}C HSQC spectra of the pretreated extract allows us to identify the major biopolymer components which are solubilized (Fig. 4B and C). The extract contains a lignin with mostly S monomers and minor quantities of guaiacyl (G) and *p*-hydroxybenzoyl (*p*HB) moieties. The βO-4 motif is the major assigned linkage observed. This corresponds well with the literature description of most hardwood and poplar lignins.[19,39,40] There is a minimal appearance of resinol or phenylcoumaran linkages but both are observable in small quantities. Some free cinnamyl alcohol groups can also be observed in concentrated extract. It has been reported that

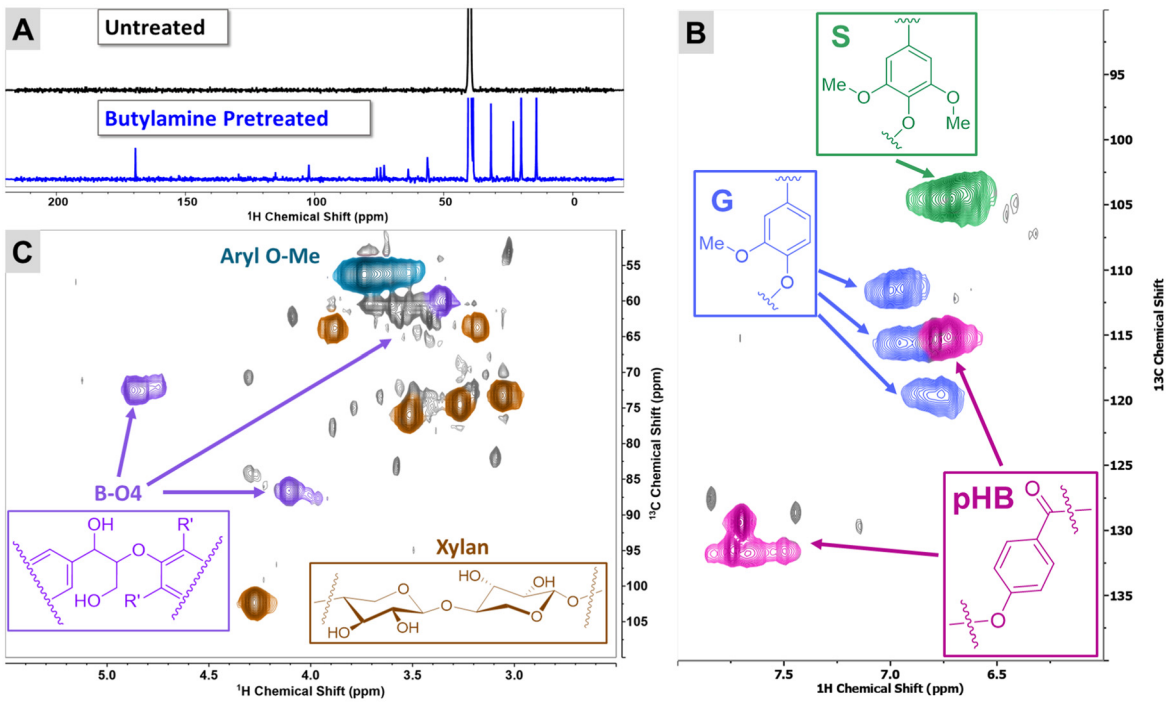

Fig. 4 ^{13}C NMR spectra of untreated and pretreated hybrid poplar extracted with DMSO-d_6 (A) and ^{1}H–^{13}C HSQC of the butylamine pretreated sample shown in the aromatic region (B) and the carbohydrate region. (C) HSQC spectra are color coded when major identifiable linkages and structural motifs when confidently assigned. Syringyl subunits (green), guaiacyl units (blue) and *para*-hydroxybenzoyl units (magenta) appear in the aromatic region, and B-O4 linkages (purple), xylan (brown) and aryl O-Me groups (teal) appear in the aliphatic region.

lignin synthesized from *p*-hydroxybenzoylated syringyl alcohol subunits produces unique β–β linkages which we suspect may be present in this lignin fraction, however we could not assign their resonances without appropriate reference compounds due to heavy overlap with reported lignin carbohydrate complexes.[41–43]

The DMSO-D_6 extract also contains some xylan, indicating some release of some hemicellulose after pretreatment. It is unclear at this point if this xylan is covalently bound to the released lignin, although some phenolic glycoside linkages could be detected at 4.71 ppm/99.29 ppm. These results indicate that both lignin and hemicellulose portions of the biomass have been made soluble by the pretreatment reaction, demonstrating a marked difference in chemical behavior between the untreated and pretreated biomass.

Additionally, we examined the DMSO-D_6 extracts of samples pretreated with 50 wt% aqueous butylamine to observe some of the changes to the reaction space when water was included in the pretreatment (Fig. S16†). The aqueous pretreated sample showed higher relative concentrations of *p*-hydroxybenzoic acid and acetic acid *versus* their respective *n*-butyl amides. This demonstrates a preference for hydrolytic ester cleavage over amidation in the aqueous condition. This suggests that higher water content pretreatments may minimize the direct chemical reactions between butylamine and the biomass, enabling more efficient solvent removal and recovery. Additionally the aqueous sample showed a higher solubilization of hemicellulosic components, suggesting that the inclusion of water aided in the dissolution and release of the polysaccharide components. This is likely due to the increased polarity of the mixed aqueous solvent *versus* neat butylamine.

Studying the DMSO extracts hints at some chemical changes in the biomass which may explain the dramatic differences in solubility. We also wanted to clarify which species were dissolving into the butylamine during the pretreatment reaction *versus* simply being released. To do this, we conducted a typical pretreatment with 15% biomass in butylamine at 140 °C for 3 hours. Instead of evaporating the butylamine to give a dry pretreated biomass, the slurry was press filtered through a 0.2 μm PTFE syringe filter to collect a butylamine filtrate. This filtrate was then concentrated *in vacuo* and NMR samples prepared from the residual solids. The residual solids after press filtration were also washed several times with butylamine to remove any other soluble components. The DMSO-d_6 extraction protocol was repeated to identify any "released" components which were not actively dissolved in the butylamine during pretreatment. The results of this are displayed in Fig. 5. The dominant component dissolved by the butylamine pretreatment is lignin, with a small fraction of xylan. It is still unclear if this xylan is part of a covalent lignin–carbohydrate complex (LCC), or simply free hemicellulose. The released material in the residual solid is a clean xylan fraction with little trace of aromatic moieties. In both extraction studies, there was a substantial concentration of components with *N*-butyl tail groups visible in the alkyl region of the HSQC spectra, providing evidence of butylamine inclusion into the

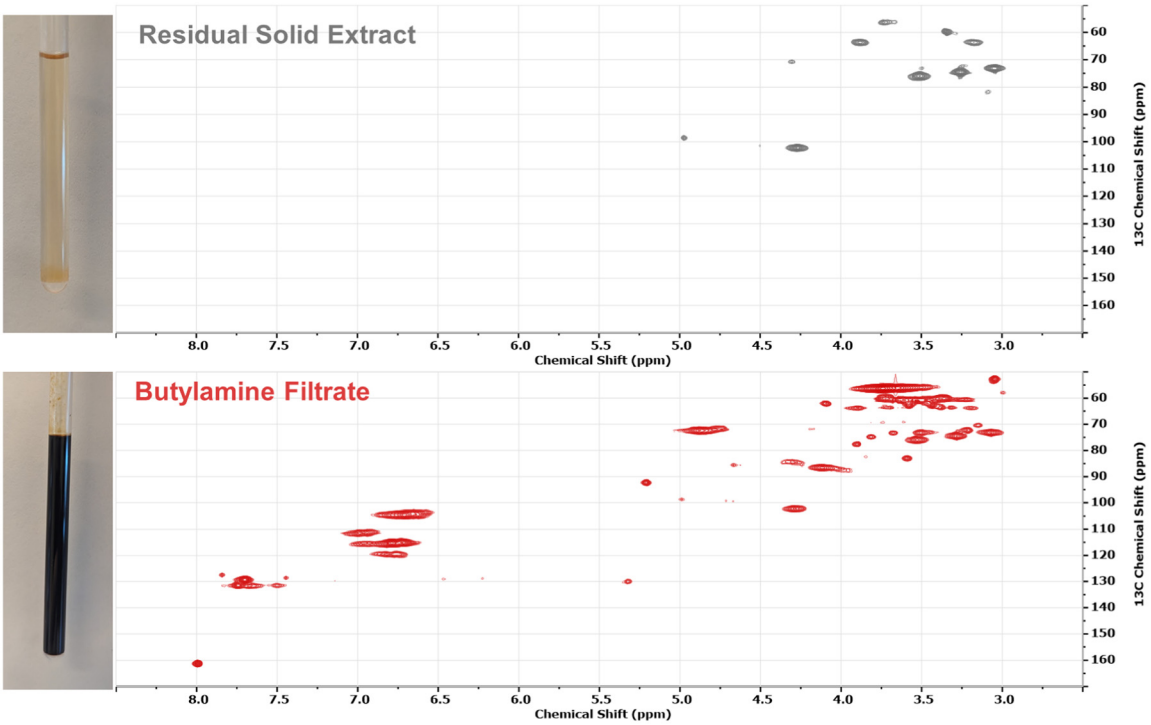

Fig. 5 $^{1}H–^{13}C$ HSQC spectra taken in DMSO-d_6 of the residual solid resulting from press filtering the wet pretreatment slurry (top, grey) and the contents of the butylamine filtrate (bottom, red).

Table 1 Elemental analysis of hybrid poplar before and after pretreatment

Untreated poplar		Butylamine pretreated poplar	
C	44.935 ± 0.205%	C	47.533 ± 0.145%
H	6.590 ± 0.334%	H	7.529 ± 0.428%
N	0.339 ± 0.100%	N	1.972 ± 0.091%
S	0.000 ± 0.000%	S	0.000 ± 0.000%

pretreated biomass. Elemental analysis of the biomass before and after pretreatment (Table 1) reveals a significant increase in the nitrogen content of the pretreated biomass, increasing from 0.339 ± 0.100% to 1.972 ± 0.091%. Since these results were obtained after extensive drying of the biomass under elevated temperature and vacuum we hypothesized that this nitrogen was likely in the form of non-volatile derivatives of butylamine, rather than trapped solvent.

To explore the nature of the residual butylamine derivatives, we used LC-MS to investigate the major organic soluble small-molecule products. The results from this are shown in Table 2. The major detected compounds were *n*-butylamine, *N*-butylacetamide, *N*-butyl-4-hydroxybenzamide (*p*HBAmide) and 4-((butylimino)methyl)phenol. The major detected acid was 4-hydroxybenzoic acid (*p*HBA), with trace (<1 μM) quan-

Table 2 LC-MS analysis of the major nitrogen containing (top), and acid/aldehyde (bottom) small molecules detected in an acetonitrile extract of butylamine pretreated hybrid poplar

Assigned compound	Structure	Concentration (μM)	Formula	Observed *m*/*z*	RT
Amines, amides and imines					
n-Butylamine	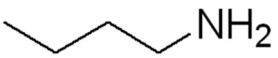	421.148	$C_4H_{11}N$	73.09	1.82
N-Butylacetamide	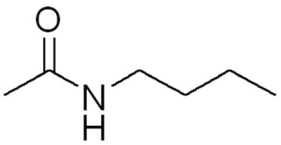	1291.408	$C_6H_{13}NO$	115.1	3.3
N-Butyl-4-hydroxybenzamide	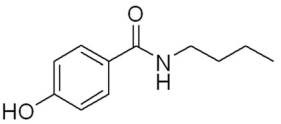	97.100	$C_{11}H_{15}NO_2$	193.111	5.26
4-((Butylimino)methyl)phenol	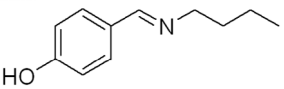	22.956	$C_{11}H_{15}NO$	177.115	7.06
Acids and aldehydes					
4-Hydroxybenzoic acid	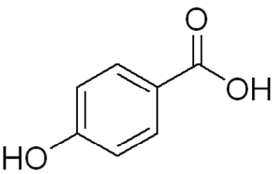	19.525	$C_7H_6O_3$	138.031	2.93
4-Hydroxybenzaldehyde	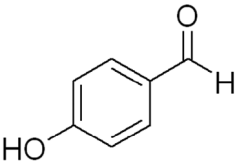	1.234	$C_7H_6O_2$	122.037	3.86
Protocatechuic acid	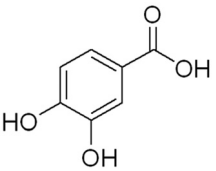	1.743	$C_7H_6O_4$	154.024	2.48
Salicylic acid	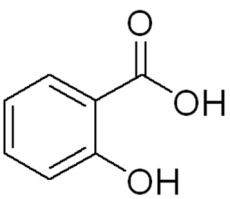	0.517	$C_7H_6O_3$	138.031	5.4

tities of 4-hydroxybenzaldehyde, protocatechuic acid and salicylic acid detected.

N-Butylacetamide occurring in the highest concentration is unsurprising. Hardwood hemicellulose is reported to have a concentration of acetylated monosaccharides[44] which we can expect to be cleaved under amidation conditions. While we did not include quantification of acetyl groups in the compositional analysis, the 1291 μM is consistent with a 1–3% acetyl group content in the starting biomass which falls within a typical range for hardwood samples. The high boiling point of the acetamide explains why it remains in the dried biomass in higher concentrations than residual *n*-butylamine, which we suspect is a combination of physisorbed and chemisorbed in the biomass. The detection of *p*HBA and *p*HBAmide in relative concentrations of 19.525 μM and 97.100 μM respectively demonstrates both the successful cleavage of the lignin-esters, as well as the dominance of the amidation chemistry over hydrolysis under these conditions. 4-Hydroxybenzaldehyde is a known oxidative decomposition product of poplar lignin,[45] and the high reactivity of aldehydes towards primary amines provides a convincing explanation of the detection of the 4-((butylimino)methyl)phenol.

To verify the observation of these compounds, *N*-butylacetamide, *N*-butyl-4-hydroxybenzamide and 4-((butylimino)methyl)phenol were prepared synthetically to use as standards for LC-MS, 1D and 2D NMR experiments and were used to validate their presence in the HSQC and HMBC spectra of the pretreated extracts discussed earlier.

Infrared spectroscopy further reveals the extent of this amidation chemistry (Fig. 6). Untreated hybrid poplar samples show a strong absorption feature at 1733 cm^{-1} which can be assigned to the C=O stretch of ester moieties throughout the biomass. Following butylamine pretreatment we observe a complete loss of this feature. Two prominent new features appear in the spectra of pretreated biomass. Centered around 1638 cm^{-1} and 1559 cm^{-1} we assign them as the C=O stretch and N–H bend of the *n*-butyl amides. This supports the previous observation of small-molecule amides within the extracts of pretreated biomass, but also demonstrates that most, if not all, of the ester functionality is cleaved during the pretreatment reaction.

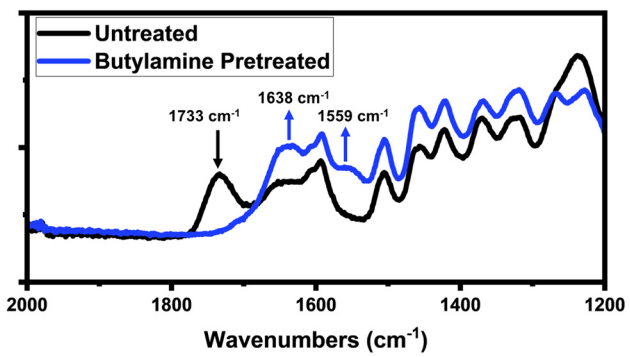

Fig. 6 ATR-FTIR of untreated (black) and butylamine pretreated (blue) hybrid poplar samples showcasing the loss of the 1733 cm^{-1} ester stretching peak in the untreated biomass, and the appearance modes at 1638 cm^{-1} and 1559 cm^{-1} which are assigned to amide C=O stretching and N–H bending respectively.

This pervasive ester cleavage mirrors the behavior of ammonia based pretreatments, however previous protocols showed much more extensive cellulose disruption than what we have observed with this butylamine pretreatment.[15,18–20] The high sugar release we were able to obtain with this pretreatment strategy allows us to postulate that the disruption of cellulose crystallinity may be an unnecessary step in biomass pretreatment. Although some reports have suggested deacetylation of biomass is a vital pretreatment step,[46] we find it difficult to conclude that the simple removal of clip-off components from the lignin and hemicellulose would result in such dramatic differences in solubility of the lignin and hemicellulose before and after pretreatment. An alternative hypothesis is that deacetylation is diagnostic of concomitant structural ester cleavage which is the true transformation necessary for effective pretreatment. Monolignol conjugates have been demonstrated to play a vital role in the synthesis of lignin within the cell wall,[47] although the specific role of *p*-hydroxybenzoyl (*p*HB) conjugates has remained elusive. γ-Esters of uronic acids in hemicellulose have been repeatedly observed in hardwood lignin–carbohydrate complexes and are a known cross-linkage motif within biomass.[36,37,48–52] There is evidence that *p*HB conjugates play an important structural role in poplar lignocellulose,[53] suggesting that some ester cross-linking between *p*HB conjugates may be an additional motif in poplar cell walls. In monocots, monolignol conjugates of coumaric and ferulic acid are known cross-linkage groups between lignin and the polysaccharide fractions[47,54] so we believe it is a reasonable suspicion that *p*HB plays a similar role in hardwoods. However, truly conclusive identification of this linkage chemistry has been difficult to obtain.

To attempt to obtain evidence of cleaved lignin–lignin and lignin–hemicellulose linkages, we conducted a fractionation scheme to isolate the soluble biopolymer components from the pretreated biomass. First, pretreated poplar was washed extensively with methanol to remove soluble lignin and organic small molecules from the biomass. This methanol filtrate was then concentrated, followed by the addition of diethyl ether to induce precipitation of the lignin fraction. This precipitate was washed extensively with additional ether to remove any residual small-molecule species which previously dominated the 2D NMR spectra of the extracts. A schematic of the various sample isolation methods is shown in Fig. S17.† The resulting fraction appeared to be an isolated lignin fraction which was completely soluble in DMSO-d_6. In addition to HSQC spectra, which show the directly adjacent carbon and proton resonances in the molecule, we also employed a TOCSY : HSQC which helps to reveal connectivity between nearby protons within a bonding network.[55] This allows for the identification of linkages between two distinct moieties within biomass, as evidenced by the appearance of cross-peaks between signals in the traditional HSQC spectra.

The aromatic region of the HSQC and TOCSY : HSQC of this fraction are shown in Fig. 7A. The HSQC of this fraction reveals that there is a substantial amount of *p*HB moieties remaining in the biomass. Because this broad *p*HB feature is distinct from both *p*HBA and *p*HBAmide reference compounds, and it remains with the precipitated lignin fraction even after extensive washing, we can only conclude that these *p*HB moieties are still directly bound to the lignin. This is further evidenced by the broadness of this feature in the ^{1}H dimension. The TOCSY : HSQC reveals cross peaks with the *p*HB proton signal at 7.80 ppm with carbons at 38.58 and 31.65 which assign to the C_1 and C_2 carbons of the *N*-butyl amide of lignin bound *p*HB. We take this as strong evidence that butylamine has cleaved the acyl functionality of these groups in the native biomass.

From the previous FTIR results it appears that most ester linkages have been cleaved during pretreatment, which suggests that these residual *p*HB groups are likely etherified with the lignin. We propose that the likely linkage sites are either in the α or β ether position of the lignin subunits. This will need to be studied more in depth with ^{13}C enriched biomass to make the identification of the exact attachment chemistries conclusive. Discussion of ether linked *p*HB has been quite limited, as it is typically only referenced as a "clip-off" compound, but this result suggests that *p*HB may play a larger role as a branch point for lignin polymerization. This theory may help explain the dramatic differences in lignin solubility before and after pretreatment, as cleavage of the branching groups leads to linear lignin which may be more easily solubilized. To study the water soluble biopolymers, the pretreated and methanol washed biomass was then extracted extensively with warm water (60 °C) over several days to generate an aqueous filtrate which is rich in water soluble hemicelluloses. The combined aqueous extract was then dried and redissolved in D_2O. The HSQC of this fraction is shown in Fig. 7B and C. The resulting fraction is expectedly rich in water soluble polysaccharides, with the major identifiable component being deacetylated glucuronoxylan.[56,57] Ester linkages between glucuronic acid and lignin have been established previously.[48,49,52] We suspect that the cleavage of this ester linkage by butylamine is important for the release of hemicellulose during pretreatment. Between 3.2–2.7 ppm/39 ppm in the ^{1}H/^{13}C dimensions, there is a strong signal which we assign as the alpha carbon of various *n*-butylated moieties. Unfortunately the solubility of this fraction was minimal enough that direct amidation of any suspected uronic acids was also not observable. The unexpected inclusion of some *p*HB moieties in this hemicellulose fraction may suggest that *p*HB may also serve as a lignin–hemicellulose cross-linkage motif in a similar fashion to ferulic acid in other angiosperms,[54,58] however this will certainly need to be studied further to give the claim more substance. If true, it may imply a multifaceted structural role of *p*HB in the cross-linkages between the various components of hardwood lignocellulose.

These results allow us to propose a mechanistic picture of the butylamine pretreatment of hybrid poplar. As the butylamine permeates into the lignocellulose matrix, cleavage of ester cross-linkages between the interconnected biopolymers facilitates the release and physical separation of the lignin and polysaccharide components of the biomass. This release and dissolution allows the cellulase and hemicellulase enzymes

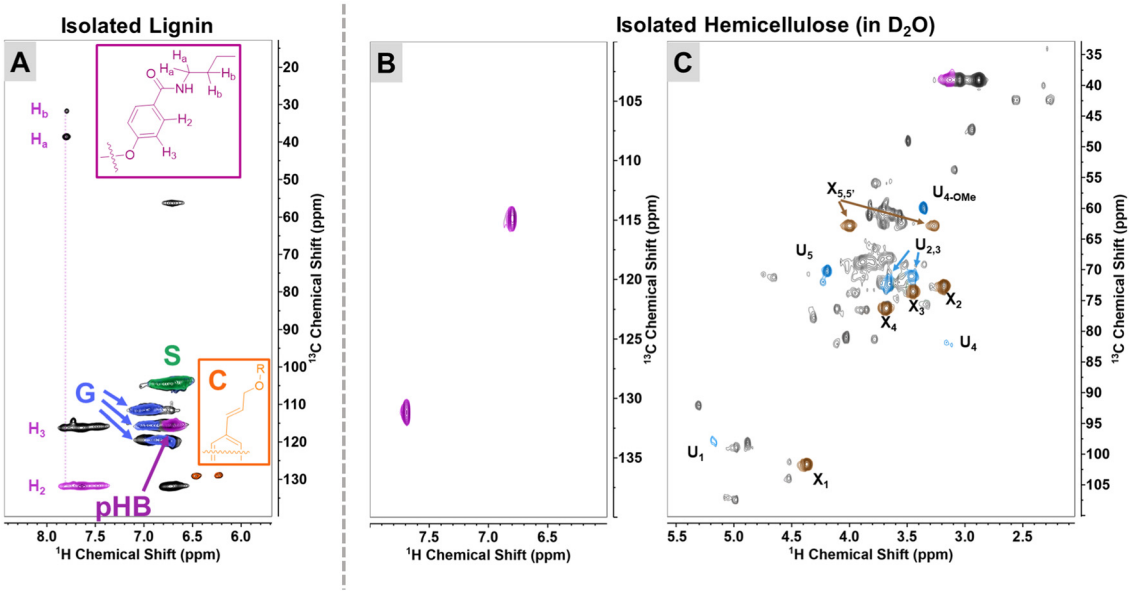

Fig. 7 Overlaid ^{1}H–^{13}C HSQC (colored) and TOCSY : HSQC (black) spectra (A) of the ether precipitated lignin fraction dissolved in DMSO-d_6. Syringyl subunits (green), guaiacyl subunits (blue), *p*-hydroxybenzoyl subunits (magenta) and residual cinnamyl alcohol moieties (orange) are labelled by color. ^{1}H–^{13}C HSQC of the hemicellulose rich aqueous filtrate shown in the aromatic region (B) and the aliphatic region.(C) X_n labels mark the resonances associated with linear xylan chains, (brown) and U_n labels mark peaks associated with xylan bound 4-methyl-glucuronic acid (teal).

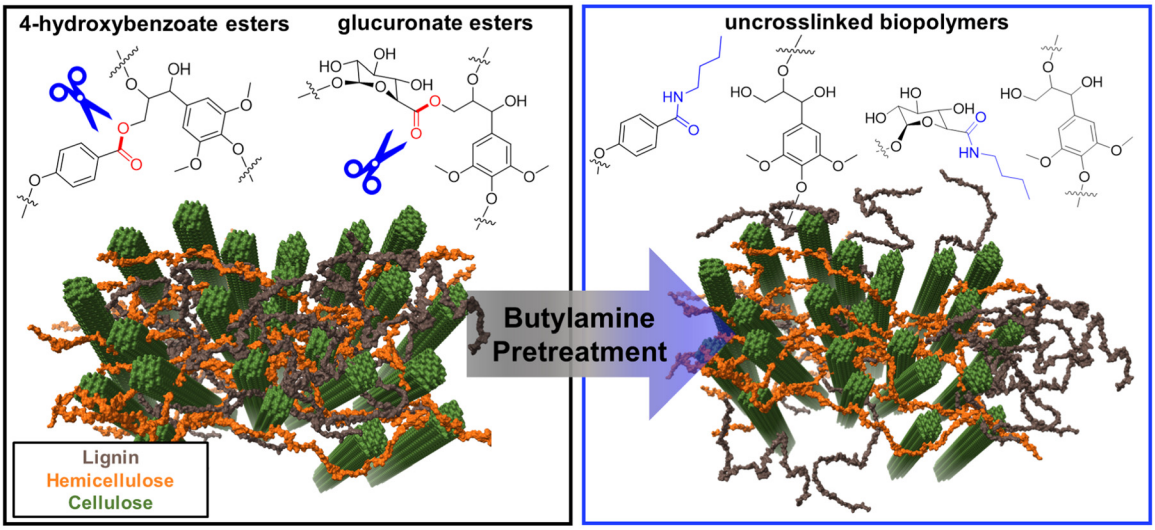

Scheme 2 Diagram of proposed mechanism of butylamine pretreatment, showing *p*HB and glucuronate ester cross-linkages (left) and the cleaved amidation products (right). Below shows the proposed structural changes to lignocellulose after the lignin (grey) has been released from the interconnected structure of cellulose (green) and hemicellulose (orange).

access to begin digestion of glycosidic linkages. A visualization of this proposed mechanism is shown in Scheme 2.

Conclusions

In this work we demonstrate the high efficacy of butylamine as a pretreatment solvent for hybrid poplar. The butylamine can be effectively removed from the biomass by evaporation, providing a viable route for future solvent recycling efforts. We explore the material and chemical effects the butylamine pretreatment has on the properties of lignocellulose. We find that butylamine serves as a targeted pretreatment solvent, showing little signs of cellulose dissolution, decrystallization and minimal alteration of the macrostructure of the biomass samples.

The main evidence of pretreatment appears in the increased solubility of lignin, and the cleavage of ester linkages within the biomass. These results suggest a mechanism which involves butylamine permeation into the lignocellulose, followed by ester cleavage, and the release of lignin from the matrix. The concomitant release of clip-off phenolics and acetate groups may provide a route for isolation of fine-chemical fractions directly from a pretreatment process. The detailed study of the structures of hybrid poplar biomass before and after pretreatment suggests that 4-hydroxybenzoate esters in biomass may act as branch points or cross-linkers within lignocellulose, and the breakage of those ester linkages provides a tractable mechanism to unravel the lignocellulose network. This importance of ester cleavage on the pretreatment process will allow us to pursue more facile, and scalable lignocellulose deconstruction chemistries which can target lignocellulose cross-linkages at lower temperatures, concentrations and with non-toxic reagents.

While a fundamental understanding of pretreatment chemistry is important, there are many additional steps necessary to establish butylamine, or other amine, pretreatments as viable processes for large-scale utilization. Lab and pilot scale demonstrations of solvent recycling will be essential for establishing the limits of solvent reuse, nitrogen loss to side-reactions, and obtaining realistic technoeconomic analysis of the energetics and costs of the process. While the high reactivity of butylamine enables efficient pretreatment, its reactivity and toxicity are very important considerations. The high volatility of butylamine provides the benefit of lowering the energy cost of the solvent recovery process,[59] however with higher volatility comes a higher flammability risk. Because this pretreatment showed promising results under high aqueous loadings, this may assist with mitigating those risks, and additionally improve downstream toxicity issues by favoring hydrolysis reactions over amidation chemistry.[60] Full optimization and exploration of the aqueous amine space will be an important area of study. Dilution of the pretreatment solvent with residual moisture from the feedstock biomass, will require clever process design to maintain pretreatment efficacy over many solvent reuse cycles.

While this work shows butylamine to be very effective for pretreatment of hybrid poplar, many of the downstream process considerations may favor the selection of other alkylamines. We expect the mechanistic results from this work will be applicable to the whole family of alkylamine pretreatment reagents. We also believe this ester cleavage mechanism can be extrapolated to other angiosperm feedstocks (bamboo, corn, rice, switchgrass, sugarcane, *etc.*) which also feature prominent ester cross-linkages within the cell wall structure. This understanding lets us approach a pretreatment chemistry which can unlock a wide variety of plant biomass for chemical and biological biorefinery processes.

Experimental methods

Hybrid poplar sourcing and pre-processing

Hybrid poplar samples were obtained from Idaho National Laboratory (sample ID 4e9a41fd-c55a-a65a-fd7b36cc0aaa). The samples were sourced from the Boardman Tree Farm in Morrow County, Oregon managed by Greenwood Resources and handled and inventoried by Idaho National Laboratory. The hybrid is a cross between *Populus deltoides* and *Populus nigra* with clone OP 367 (433). The samples were ground using a knife mill with a round slit 2 mm outlet screen. The milled sample was allowed to air dry until the total moisture content of the sawdust was repeatedly measured under 10%. The sample was stored in a cool dark environment and used without any further processing.

Butylamine pretreatment of hybrid poplar (tube scale)

Following previously established protocols,[25,59] hybrid poplar (300 mg) was placed in a tared tube flask. Pretreatment solvent (1.7 g butylamine or butylamine : water solutions) was then added and the vessel was sealed with a Teflon stopper. The tube was placed in an oil-bath preheated to 140 °C for 3 hours. After the allotted time the tube flasks were removed from the oil bath, allowed to cool for 30 minutes, before the stopper was removed and the flasks transferred to a vacuum oven. The pretreated samples were then dried at 80 degrees celsius under house vacuum for at least 12 hours. After drying the tube + dried biomass was weighed again, and the residual dry biomass weight was used to determine the amount of solvent removed by evaporation.

Butylamine pretreatment of hybrid poplar (75 mL Parr scale)

Reactions under controlled atmosphere were run in a Parr instrument company series 5000 multiple reactor system. The reactor vessels used had a total volume of 75 mL and were fitted with a thermostat, pressure sensor and rupture disk with a pressure rating of 200 psi. Reactions were set up by loading 1.5 g of untreated biomass, 8.5 g of butylamine and a Teflon stir bar into the reactor. The atmosphere was exchanged 5 times with 1 bar N_2, O_2 or CO_2 before the reactors were closed. The stirring speed was set to 200 rpm. The reactors were brought to temperature (140 °C) before being allowed to stir at temperature for 3 hours before being allowed to cool to room temperature. The reactors were then opened, covered with a kimwipe, and dried in a vacuum oven at 80 °C overnight.

Butylamine pretreatment of hybrid poplar (1 L Parr scale)

A 1 L 4520 Parr bench-top reactor (Parr Instrument Company, Moline, IL) was used to prepare larger quantities of butylamine pretreated biomass. 30 g of poplar was mixed with 170 g of butylamine. The reactors were stirred at 75 rpm, and heated to 140 °C for 3 hours. The mixtures were vacuum-dried at 80 °C following pretreatment, and the weights were recorded at each stage. The dried pretreated biomass was then used for the characterization of pretreated biomass.

Fractionation protocol to isolate poplar lignin and hemicellulose

12 g of pretreated hybrid poplar biomass was suspended in 250 mL of methanol in a round bottom flask and stirred for 24 hours. The solid was filtered, and returned to the flask for two more identical washing steps. After the final washing with methanol the solid was dried under vacuum to remove any residual methanol, before being resuspended in 250 mL of warm water (60 °C) for 24 hours. The slurry was again sequentially filtered and washed with water a total of three times and the aqueous filtrates were combined and dried *in vacuo* to result in the hemicellulose rich fraction shown in Fig. 7B and C.

The methanol filtrates from the first washing steps were combined and concentrated *in vacuo*. The resulting concentrate was a dark brown oil, which was resuspended in methanol until homogeneous. The mixture was then diluted with diethyl ether, resulting in a beige precipitate which was left to settle for 1 hour. The solid was then filtered and dried further under vacuum at 80 °C. This solid was then used as the isolated lignin fraction shown in Fig. 7A.

Enzymatic hydrolysis protocol

Once the biomass was sufficiently dried to remove major traces of butylamine, the biomass was rehydrated with 1.4 mL deionized water for every 300 mg of biomass. This slurry was agitated and allowed to rest for at least 30 minutes to ensure full hydration. The pH of the resulting slurry was then adjusted to within 4.75–5.25 using a 5% solution of H_2SO_4. After the pH had stabilized within the desired region, 1 M citric acid buffer (pH 5, 100 μL/300 mg biomass), 2% sodium azide (100 μL/300 mg biomass), and enzyme solution (novozymes HTEC3 : CTEC3 9 : 1 ratio diluted with distilled water to 100 μL/300 mg biomass) were added. The dilution of the enzyme cocktail (with a CTec 3 : HTec 3 ratio of 9 : 1 by volume from Novozymes) was adjusted to ensure a 15% dry solids loading of the slurry with 30 mg of enzymes per gram of biomass. The samples were incubated under agitation for 3 days at 50 °C.

Preparation of reference compounds for NMR and HP-LC analysis

N-Butylacetamide was prepared by refluxing butylamine in acetic acid overnight with a catalytic amount of $Zn(OAc)_2$ as reported by Brahmachari and coworkers.[61] *N*-Butyl-4-hydroxybenzamide was prepared from methyl-4-hydroxybenzoate as reported by Aitken *et al.*[62] 4-((Butylimino)methyl)phenol was prepared from 4-hydroxybenzaldehyde with an equimolar amount of butylamine as reported by Marchand *et al.*[63] All compounds matched their reported syntheses and characterization.

Characterization methods

HPLC method for the quantification of monosaccharides. The concentrations of monomeric sugars (glucose and xylose)

in the resulting hydrolysate after enzymatic digestion of pretreated biomass were determined by HPLC using an Agilent 1200 series instrument equipped with a Bio-Rad Aminex HPX-87H column and a refractive index detector. An aqueous solution of 4 mM H_2SO_4 was used as the mobile phase (column temperature 60 °C, 0.6 mL min^{-1}) for the separation of products. The total run time was set to 20 min and the theoretical yields from glucan and xylan were calculated from the glucose and xylose content adjusted by the correction factors of 162/180 and 132/150, respectively to adjust for the rehydration of the monosaccharides.

Powder X-Ray diffraction. The untreated and pretreated biomass samples were dried thoroughly under vacuum at 80 °C for 48 hours and analyzed without any additional processing steps to avoid altering the samples material properties. The pXRD spectra were taken on a Rigaku Miniflex 6x Benchtop Powder XRD instrument operating with a sealed Cu-Kα source tube and a HyPix-400MF Hybrid Pixel Array detector.

Thermal gravimetric analysis. TGA measurements were performed on a Mettler Toledo TGA/DSC 3+ thermogravimetric analyzer. Approximately 10 mg of sample was added to an aluminum sample tray for each run. The TGA curves were generated under ambient atmosphere with a temperature ramp of 10 °C per minute.

Fluorescence microscopy. Unmodified dry pretreated and untreated biomass samples were loaded onto a glass microscope slide. Fluorescence microscopy images were taken on a Leica DM6B microscope under broadband illumination with the digital acquisition platform (DAP) fluoro-cube (excitation wavelength 325–375 nm, emission wavelength 435–485 nm). Autofluorescence emitted from phenolic deposits was recorded using a Leica-DMC4500-0042671016 camera and the signal was provided with a pseudo-color, cyan. The UV autofluorescence signals of the biomass before and after pretreatment were measured using the Las X Leica software by selecting the area showing autofluorescence. Quantifications of fluorescence intensity were normalized per micrometer of region of interest (ROI), and to maintain homogeneity in the process, the images for both pretreated and untreated samples were presented using identical contrast parameters.

Solution state NMR. NMR extract samples of pretreated biomass were prepared by combining ~100 mg of dried biomass material with 1 mL of DMSO-d_6 before immersing in an ultrasonic bath for 10 minutes. All samples had at least 6 hours between sample preparation and spectrum collation. All 2D experiments (HSQC, HMBC, TOCSY : HSQC) were collected on a Bruker AVANCE NEO 500 MHz instrument equipped with a 5 mm BBO Prodigy CryoProbe utilizing previously reported pulse programs.[51] Other 1D experiments were run on a 400 MHz JEOL instrument with a ECZL400S console and a 5 mm HFX probe. 2D spectra were processed with 20 Hz exponential and a 90° sin squared apodization factors in both dimensions and baselined with a full automatic Whittaker Smoother protocol in both dimensions using MestReNova version 15.0.1. 2D spectra were referenced using the solvent residual signal of DMSO-d_6 appearing at 39.52 ppm in the ^{13}C dimension and 2.50 ppm in the ^{1}H dimension.

Solid state CP-MAS NMR. ^{13}C solid-state NMR (ssNMR) spectra were recorded at B_0 = 11.75 T (500.1 MHz for ^{1}H) using a Bruker BioSpin spectrometer equipped with an AVANCE-I console and 4.0 mm double resonance HX magic angle spinning (MAS) probes tune to both ^{1}H (500.1 MHz) and ^{13}C (125.76 MHz). Dried biomass samples were first ball-milled using a Retsch Mixer Mill MM 500 vario using a cycle of 5 minutes shaking at 30 Hz followed by a 10 minutes downtime to avoid sample overheating. This cycle was looped 5 times until the samples were a free-flowing powder. The samples were packed into a 4 mm zirconia rotor with a Kel-F cap. All samples were spun at 10 kHz using dry nitrogen unless otherwise stated. ^{13}C chemical shift was referenced with respect to tetramethylsilane using the CH resonance of adamantane as a secondary external reference at $\delta_{iso}(^{13}C)$ = 38.48 ppm. ^{13}C ssNMR spectra were obtained using a $^{1}H \rightarrow {}^{13}C$ cross-polarization (CP) transfer under MAS (CP-MAS). The CP-MAS experiments used a constant radio frequency field (RF-field) equal to 38 kHz was applied on the ^{13}C, while the ^{1}H RF-field amplitude was linearly ramped from 49.1 to 54.5 kHz. During ^{13}C acquisition, high-power ^{1}H decoupling was applied using the SPINAL-64 (Small Phase Incremental Alternation with 64 steps)[64] decoupling scheme with an RF-field amplitude set to 54.5 kHz. A total of 256 transients were averaged with a repetition time of 2 s resulting in experimental times of 9 min. All reported CP-MAS spectra were collected with a 1 ms cross polarization duration, which was determined to be sufficient to show intensity in all regions of interest in the ^{13}C spectrum. All solid-state NMR data were processed using Bruker TopSpin 4.4.0.

Elemental analysis. Dried biomass samples were first ball-milled using a Retsch Mixer Mill MM 500 vario using a cycle of 5 minutes shaking at 30 Hz followed by a 10 minutes downtime to avoid sample overheating. This cycle was looped 5 times until the samples were observed as a free-flowing powder. Samples were then submitted to the UC Berkeley Microanalytical facility for CHNS analysis. Samples were run in triplicate on a ThermoFisher Flash Smart Elemental analyzer and reported as the average of the three runs.

LC-MS of pretreated poplar extract. Extracts of pretreated biomass for analysis by LC-MS were prepared by suspending dried pretreated hybrid poplar (100 mg) in acetonitrile (20 mL) before agitating for 10 minutes in an ultrasonic cleaning bath. The mixture was then passed through a 0.2 μm PTFE syringe filter to generate a solid-free organic extract of the pretreated biomass. Butylamine and the other analytes were quantified by the LC-MS method described previously.[65]

Compositional analysis of poplar samples. The chemical composition of the raw biomass was analyzed using a method adapted from the NREL LAP protocol.[28] In this procedure, 300 mg of finely ground sample was treated with 3 mL of 72% H_2SO_4 in a serum bottle at 30 °C for 1 hour. Following the initial acid hydrolysis, the mixture was diluted to a 4% acid concentration by adding 84 mL of deionized water. The

diluted mixture then underwent a second acid hydrolysis stage by autoclaving at 121 °C for 60 minutes. The acid-insoluble lignin content was determined gravimetrically using tared Gooch filtering crucibles (Medium Porosity, DWK Life Sciences Kimble™ KIMAX™, Millville, NJ). After filtration, the carbohydrate content in the filtrate was analyzed using an Ultimate 3000 high-performance liquid chromatography (HPLC) system equipped with a refractive index detector (Thermo Scientific, Waltham, MA, USA). An Aminex HPX-87H column (300 × 7.8 mm, Bio-Rad, Hercules, CA, USA) was employed, with 4 mM sulfuric acid as the mobile phase at a flow rate of 0.6 mL min^{-1}. The column oven was maintained at 60 °C. The acid-soluble lignin in the filtrate was measured at 240 nm using a UV/Vis spectrophotometer (Nanodrop 2000, Thermo Scientific, USA). Subsequently, the residue was transferred to a muffle furnace and subjected to heating at 575 °C for an additional 6 hours. Crucibles were allowed to cool in desiccators, and their weights were recorded between each heating interval.

The moisture content of the raw biomass was evaluated by drying 0.5 to 2 grams of the sample in porcelain crucibles using a conventional oven (Binder GmbH, Germany) for 18–24 hours. The dried biomass was subjected to further heating in a muffle furnace at 575 °C for at least 6 hours to determine the ash content. Crucibles were permitted to cool in desiccators, and their weights were recorded between each heating phase.

Moisture content % of biomass:

$$\text{Moisture content}\,\% = \frac{(\text{weight of the wet biomass (g)} - \text{weight of the dried biomass (g)})}{\text{weight of wet biomass (g)}} \times 100. \quad (1)$$

Ash content % of biomass:

$$\text{Ash content}\,\% = \frac{(\text{weight of the wet biomass (g)} - \text{weight of ashed biomass (g)})}{\text{weight of wet biomass (g)}} \times 100. \quad (2)$$

Data availability

The authors declare that the data supporting the findings of this study are available within the paper and its ESI.† Should any raw data files be needed in another format they are available from the corresponding author upon reasonable request.

Conflicts of interest

BAS has a financial interest in Illium Technologies, Caribou Biofuels, and Erg Bio. XC, AK, JMP, VRP, and BAS are named inventors on at least one related patent application. All other authors have no financial interest to disclose.

Acknowledgements

This work was supported by the DOD Tri-Service Biotechnology for a Resilient Supply Chain (T-BRSC) program through award AWD00007196 to Lawrence Berkeley National Laboratory. The portion of the work conducted at the Joint BioEnergy Institute was supported by the U.S. Department of Energy, Office of Science, Biological and Environmental Research Program, through contract DE-AC02-05CH11231 between Lawrence Berkeley National Laboratory and the U.S. Department of Energy. The portion of the work conducted at the Advanced Biofuels and Bioproducts Development Unit was supported by the U.S. Department of Energy, Office of Energy Efficiency and Renewable Energy, Bioenergy Technologies Office. We thank Dr Hasan Celik and Pines Magnetic Resonance Center's Core NMR Facility (PMRC Core) for spectroscopic assistance. The instruments used in this work were supported by the PMRC Core. We thank Nick Setterini for assistance collecting the powder X-ray diffraction spectra. Sandia National Laboratories, a multimission laboratory managed and operated by National Technology and Engineering Solutions of Sandia LLC, a wholly owned subsidiary of Honeywell International Inc. for the U.S. Department of Energy's National Nuclear Security Administration under contract DE-NA0003525. The United States Government retains and the publisher, by accepting the article for publication, acknowledges that the United States Government retains a nonexclusive, paid-up, irrevocable, worldwide license to publish or reproduce the published form of this manuscript, or allow others to do so, for United States Government purposes. Any subjective views or opinions that might be expressed in this paper do not necessarily represent the views of the U.S. Department of Energy, U.S. Department of Defense, or the United States Government.

References

1 C. Somerville, *Science*, 2006, **312**, 1277–1277.
2 M. Langholtz, Oak Ridge National Laboratory (ORNL), Oak Ridge, TN (United States), Bioenergy Knowledge Discovery Framework (BEKDF); Oak Ridge National Laboratory (ORNL), Oak Ridge, TN (United States), Bioenergy Knowledge Discovery Framework (BEKDF), DOI: 10.23720/bt2023/2316165.
3 D. M. Morris, R. L. Quintana and B. G. Harvey, *ChemSusChem*, 2019, **12**, 1646–1652.
4 K. E. Rosenkoetter, C. R. Kennedy, P. J. Chirik and B. G. Harvey, *Green Chem.*, 2019, **21**, 5616–5623.
5 N. R. Baral, M. Yang, B. G. Harvey, B. A. Simmons, A. Mukhopadhyay, T. S. Lee and C. D. Scown, *ACS Sustainable Chem. Eng.*, 2021, **9**, 11872–11882.

6 C.-L. Liu, T. Tian, J. Alonso-Gutierrez, B. Garabedian, S. Wang, E. E. K. Baidoo, V. Benites, Y. Chen, C. J. Petzold, P. D. Adams, J. D. Keasling, T. Tan and T. S. Lee, *Biotechnol. Biofuels*, 2018, **11**, 285.
7 J. S. Van Dyk and B. I. Pletschke, *Biotechnol. Adv.*, 2012, **30**, 1458–1480.
8 G. Brodeur, E. Yau, K. Badal, J. Collier, K. B. Ramachandran and S. Ramakrishnan, *Enzyme Res.*, 2011, **2011**, 787532.
9 A. R. Mankar, A. Pandey, A. Modak and K. K. Pant, *Bioresour. Technol.*, 2021, **334**, 125235.
10 A. K. Chandel, V. K. Garlapati, A. K. Singh, F. A. F. Antunes and S. S. da Silva, *Bioresour. Technol.*, 2018, **264**, 370–381.
11 V. Balan, *ISRN Biotechnol.*, 2014, **2014**, 463074.
12 J. S. Kim, Y. Y. Lee and T. H. Kim, *Bioresour. Technol.*, 2016, **199**, 42–48.
13 J. Yang, M. Sun, L. Jiao and H. Dai, *Polymers*, 2021, **13**(23), 4166.
14 P. Bajpai, in *Green chemistry and sustainability in pulp and paper industry*, Springer International Publishing, Cham, 2015, pp. 11–39.
15 S. P. S. Chundawat, R. Vismeh, L. N. Sharma, J. F. Humpula, L. da Costa Sousa, C. K. Chambliss, A. D. Jones, V. Balan and B. E. Dale, *Bioresour. Technol.*, 2010, **101**, 8429–8438.
16 A. Mittal, R. Katahira, B. S. Donohoe, S. Pattathil, S. Kandemkavil, M. L. Reed, M. J. Biddy and G. T. Beckham, *ACS Sustainable Chem. Eng.*, 2017, **5**, 2544–2561.
17 J. R. Meyer, S. B. Waghmode, J. He, Y. Gao, D. Hoole, L. da Costa Sousa, V. Balan and M. B. Foston, *Biomass Bioenergy*, 2018, **119**, 446–455.
18 F. Teymouri, L. Laureano-Perez, H. Alizadeh and B. E. Dale, *Bioresour. Technol.*, 2005, **96**, 2014–2018.
19 V. Balan, L. da C. Sousa, S. P. S. Chundawat, D. Marshall, L. N. Sharma, C. K. Chambliss and B. E. Dale, *Biotechnol. Prog.*, 2009, **25**, 365–375.
20 S. P. S. Chundawat, R. K. Pal, C. Zhao, T. Campbell, F. Teymouri, J. Videto, C. Nielson, B. Wieferich, L. Sousa, B. E. Dale, V. Balan, S. Chipkar, J. Aguado, E. Burke and R. G. Ong, *J. Visualized Exp.*, 2020, **158**, e57488.
21 L. Xu, M. Cao, J. Zhou, Y. Pang, Z. Li, D. Yang, S.-Y. Leu, H. Lou, X. Pan and X. Qiu, *Nat. Commun.*, 2024, **15**, 734.
22 S. Ntakirutimana, T. Xu, H. Liu, J.-Q. Cui, Q.-J. Zong, Z.-H. Liu, B.-Z. Li and Y.-J. Yuan, *Green Chem.*, 2022, **24**, 5460–5478.
23 E. C. Achinivu, S. Frank, N. R. Baral, L. Das, M. Mohan, P. Otoupal, E. Shabir, S. Utan, C. D. Scown, B. A. Simmons and J. Gladden, *Green Chem.*, 2021, **23**, 8611–8631.
24 E. C. Achinivu, M. Mohan, H. Choudhary, L. Das, K. Huang, H. D. Magurudeniya, V. R. Pidatala, A. George, B. A. Simmons and J. M. Gladden, *Green Chem.*, 2021, **23**, 7269–7289.
25 M. Tanaka, C. W. Robinson and M. Moo-Young, *Biotechnol. Bioeng.*, 1985, **27**, 362–368.
26 P. Sannigrahi, A. J. Ragauskas and G. A. Tuskan, *Biofuels, Bioprod. Biorefin.*, 2010, **4**, 209–226.
27 T. Treasure, R. Gonzalez, H. Jameel, R. B. Phillips, S. Park and S. Kelley, *Biofuels, Bioprod. Biorefin.*, 2014, **8**, 755–769.
28 J. Sluiter, A. Sluiter, C. Scarlata, D. Templeton, D. Crocker and B. Hames, *Laboratory Analytical Procedure (LAP)*, 2012, **https://www.nrel.gov/docs/gen/fy13/42618.pdf**.
29 P. Ahvenainen, I. Kontro and K. Svedström, *Cellulose*, 2016, **23**, 1073–1086.
30 S. Singh, G. Cheng, N. Sathitsuksanoh, D. Wu, P. Varanasi, A. George, V. Balan, X. Gao, R. Kumar, B. E. Dale, C. E. Wyman and B. A. Simmons, *Front. Energy Res.*, 2014, **2**, DOI: **10.3389/fenrg.2014.00062**.
31 G. Cheng, P. Varanasi, R. Arora, V. Stavila, B. A. Simmons, M. S. Kent and S. Singh, *J. Phys. Chem. B*, 2012, **116**, 10049–10054.
32 L. da C. Sousa, J. Humpula, V. Balan, B. E. Dale and S. P. S. Chundawat, *ACS Sustainable Chem. Eng.*, 2019, **7**, 14411–14424.
33 C. Driemeier, M. T. B. Pimenta, G. J. M. Rocha, M. M. Oliveira, D. B. Mello, P. Maziero and A. R. Gonçalves, *Cellulose*, 2011, **18**, 1509–1519.
34 M. Carrier, A. Loppinet-Serani, D. Denux, J.-M. Lasnier, F. Ham-Pichavant, F. Cansell and C. Aymonier, *Biomass Bioenergy*, 2011, **35**, 298–307.
35 T. P. Schultz, G. D. McGinnis and M. S. Bertran, *J. Wood Chem. Technol.*, 1985, **5**, 543–557.
36 D. Min, C. Yang, V. Chiang, H. Jameel and H. Chang, *Fuel*, 2014, **116**, 56–62.
37 D. Min, Q. Li, V. Chiang, H. Jameel, H. Chang and L. Lucia, *Fuel*, 2014, **119**, 207–213.
38 J. Ralph and L. Landucci, in *Lignin and lignans: advances in chemistry*, ed. C. Heitner, D. Dimmel and J. Schmidt, CRC Press, 2010, pp. 137–243.
39 R. Martín-Sampedro, J. I. Santos, Ú. Fillat, B. Wicklein, M. E. Eugenio and D. Ibarra, *Int. J. Biol. Macromol.*, 2019, **126**, 18–29.
40 Y. Mottiar, S. D. Karlen, R. E. Goacher, J. Ralph and S. D. Mansfield, *Plant Biotechnol. J.*, 2023, **21**, 176–188.
41 F. Lu, J. Ralph, K. Morreel, E. Messens and W. Boerjan, *Org. Biomol. Chem.*, 2004, **2**, 2888–2890.
42 F. Lu, S. D. Karlen, M. Regner, H. Kim, S. A. Ralph, R.-C. Sun, K. Kuroda, M. A. Augustin, R. Mawson, H. Sabarez, T. Singh, G. Jimenez-Monteon, S. Zakaria, S. Hill, P. J. Harris, W. Boerjan, C. G. Wilkerson, S. D. Mansfield and J. Ralph, *Bioenerg. Res.*, 2015, **8**, 934–952.
43 T.-Q. Yuan, S.-N. Sun, F. Xu and R.-C. Sun, *J. Agric. Food Chem.*, 2011, **59**, 10604–10614.
44 S. Gille and M. Pauly, *Front. Plant Sci.*, 2012, **3**, 12.
45 W. Schutyser, J. S. Kruger, A. M. Robinson, R. Katahira, D. G. Brandner, N. S. Cleveland, A. Mittal, D. J. Peterson, R. Meilan, Y. Román-Leshkov and G. T. Beckham, *Green Chem.*, 2018, **20**, 3828–3844.
46 P. Wen, Z. Chen, Z. Lian and J. Zhang, *Bioresour. Technol.*, 2023, **385**, 129459.
47 S. D. Karlen, C. Zhang, M. L. Peck, R. A. Smith, D. Padmakshan, K. E. Helmich, H. C. A. Free, S. Lee, B. G. Smith, F. Lu, J. C. Sedbrook, R. Sibout, J. H. Grabber, T. M. Runge, K. S. Mysore, P. J. Harris, L. E. Bartley and J. Ralph, *Sci. Adv.*, 2016, **2**, e1600393.

48 J. Larsbrink and L. Lo Leggio, *Essays Biochem.*, 2023, **67**, 493–503.
49 M. L. Gandla, M. Derba-Maceluch, X. Liu, L. Gerber, E. R. Master, E. J. Mellerowicz and L. J. Jönsson, *Phytochemistry*, 2015, **112**, 210–220.
50 S.-Y. Jeong, E.-J. Lee, S.-E. Ban and J.-W. Lee, *Carbohydr. Polym.*, 2021, **270**, 118375.
51 H. Nishimura, A. Kamiya, T. Nagata, M. Katahira and T. Watanabe, *Sci. Rep.*, 2018, **8**, 6538.
52 T. Watanabe and T. Koshijima, *Agric. Biol. Chem.*, 1988, **52**, 2953–2955.
53 Y. Zhao, X.-H. Yu and C.-J. Liu, *Front. Plant Sci.*, 2021, **12**, 755576.
54 D. M. de Oliveira, A. Finger-Teixeira, T. R. Mota, V. H. Salvador, F. C. Moreira-Vilar, H. B. C. Molinari, R. A. C. Mitchell, R. Marchiosi, O. Ferrarese-Filho and W. D. dos Santos, *Plant Biotechnol. J.*, 2015, **13**, 1224–1232.
55 J. Ralph, J. M. Marita, S. A. Ralph, R. D. Hatfield, F. Lu, R. M. Ede, J. Peng and L. L. Landucci, *Advances in lignocellulosics characterization*, TAPPI Press, Atlanta, Ga, 1999, pp. 55–108.
56 P. Vincent, F. Ham-Pichavant, C. Michaud, G. Mignani, S. Mastroianni, H. Cramail and S. Grelier, *Polymers*, 2021, **13**(13), 2044.
57 J. Zhou, X. Du, S. Zhou and S. Wu, *Cellulose*, 2023, **30**, 4855–4871.
58 R. Samuel, M. Foston, N. Jiang, L. Allison and A. J. Ragauskas, *Polym. Degrad. Stab.*, 2011, **96**, 2002–2009.
59 E. C. Achinivu, B. W. Blankenship, N. R. Baral, H. Choudhary, R. Kakumanu, M. Mohan, E. E. K. Baidoo, C. D. Scown, A. George, B. A. Simmons and J. Gladden, *Chem. Eng. J.*, 2023, 147824.
60 C. Zhao, Q. Shao and S. P. S. Chundawat, *Bioresour. Technol.*, 2020, **298**, 122446.
61 G. Brahmachari, S. Laskar and S. Sarkar, *J. Chem. Res., Synop.*, 2010, **34**, 288–295.
62 R. A. Aitken, A. D. Harper, R. A. Inwood and A. M. Z. Slawin, *J. Org. Chem.*, 2022, **87**, 4692–4701.
63 P. Marchand, L. Griffe, M. Poupot, C.-O. Turrin, G. Bacquet, J.-J. Fournié, J.-P. Majoral, R. Poupot and A.-M. Caminade, *Bioorg. Med. Chem. Lett.*, 2009, **19**, 3963–3966.
64 B. M. Fung, A. K. Khitrin and K. Ermolaev, *J. Magn. Reson.*, 2000, **142**, 97–101.
65 B. Amer, R. Kakumanu, Y. Tian, A. Eudes and E. E. K. Baidoo, Targeted analysis of phenolic compounds by LC-MS, 2021 protocols.io DOI: **10.17504/protocols.io.byhcpt2w**.